SHORT REPORT

Cytoskeleton
DOI10.1002/cm.21631

Proper cytoskeleton α-tubulin distribution is concomitant to tyrosine phosphorylation during *in vitro* capacitation and acrosomal reaction in human spermatozoa

Paula Sáez-Espinosa[1,*], Mariola Ferrández-Rives[1,*], Natalia Huerta-Retamal[1], Laura Robles-Gómez[1], Jon Aizpurua[2], Alejandro Romero[1], María José Gómez-Torres[1,2]

[1] Department of Biotechnology, University of Alicante, Alicante, Spain.

[2] IVF Spain, Reproductive Medicine, Alicante, Spain.

[3] Cathedra of Human Fertility, University de Alicante, Alicante, Spain

[*] These authors contributed equally to this work.

Corresponding author:

María José Gómez-Torres

Department of Biotechnology, University of Alicante, 03080, Alicante, Spain. Tlf: +34 965903878; e-mail: mjose.gomez@ua.es

Short running title: α-tubulin and phosphotyrosine in human sperm

Acknowledgements

This research was supported by Human Fertility Cathedra of the University of Alicante, VIOGROB-186, and the project of the Ministry of Economy and Competitiveness AGL2015-70159-P.

Cytoskeleton, doi: 10.1002/cm.21631

Received: Jun 16, 2020;Revised: Aug 20, 2020;Accepted: Aug 28, 2020

Abstract

Spermatozoa motility is a key parameter during fertilization process. In this context, spermatozoa tyrosine protein phosphorylation and an appropriate cytoskeleton α-tubulin distribution are some of the most important physiological events involved in motility. However, the relationship between these two biomarkers remains poorly defined. Here, we characterized simultaneously by immunocytochemistry the α-tubulin (TUBA4A) distribution and the tyrosine phosphorylation at flagellum before capacitation, during different capacitation times (one and four hours), and after acrosome reaction induction in human spermatozoa. We found that the absence of spermatozoa phosphorylation in tyrosine residues positively and significantly correlated ($p<0.05$) with the terminal piece α-tubulin flagellar distribution in all physiological conditions. Conversely, we observed a positive significant correlation ($p<0.01$) between phosphorylated spermatozoa and continuous α-tubulin distribution in spermatozoa flagellum, independently of the physiological condition. Similarly, the subpopulation of spermatozoa with tyrosine phosphorylated and continuous α-tubulin increases with longer capacitation times and after the acrosome reaction induction. Overall, these findings provide novel insights into the post-transcriptional physiological events associated to α-tubulin and the tyrosine phosphorylation during fertilization, which present potential implications for the improvement of spermatozoa selection methods.

Keywords: Acrosome reaction; capacitation; microtubules; protein phosphorylation; spermatozoa

1. INTRODUCTION

Spermatogenesis takes place in mammalian seminiferous tubules and yields highly differentiated and specialized spermatic cells (Yanagimachi, 1994), which acquire motility during the epididimal maturation process (Eddy, 2006). However, the spermatozoa fertilizing capacity is acquired during the residence in the female reproductive tract (de Lamirande, Leclerc, & Gagnon, 1997) or using *in vitro* conditions (Edwards, Bavister, & Steptoe, 1969) by the process known as capacitation (Austin, 1951, 1952; Chang, 1951). Capacitation involves a set of physiological and structural changes that prepare the spermatozoa to perform the acrosomal reaction, releasing hydrolytic vesicles to cross the zona pellucida and finally fusing with the oocyte membrane (Eddy, 2006).

Human spermatozoa capacitation *in vitro* covers ranges from three to 24 hours (De Jonge, 2017). This wide time range is associated with the vast heterogeneity of semen samples, resulting in spermatozoa subpopulations with different degrees of functionality and membrane cholesterol content (Buffone, Doncel, Marin Briggiler, Vazquez-Levin, & Calamera, 2004; Buffone, Verstraeten, Calamera, & Doncel, 2009). Likewise, a previous study reported that spermatozoa need to capacitate for at least four hours for properly recognize the oocyte's zona pellucida (Baibakov, Boggs, Yauger, Baibakov, & Dean, 2012) and another report demonstrated that the timing of capacitation in human spermatozoa differs among men but is reproducible within each individual (Ostermeier et al., 2018).

Due to lack of transcriptional and translational activity once the spermatogenesis is finished, post-translational modifications (acetylation, glutamylation, glycylation, methylation, phosphorylation, and polyamination) further increase the spermatozoa heterogeneity and introduced specific changes that could be associated to functionality (Brohi & Huo, 2017). One of the key spermatozoa post-translational modification is the flagellum tyrosine protein phosphorylation (Naresh & Atreja, 2015; Naz & Rajesh, 2004), which is regulated by kinase A protein located at

flagellar fibrous sheath through a cAMP dependent pathway (Visconti et al., 1998). According to several studies, spermatozoa tyrosine phosphorylation is a time-dependent event and plays an outstanding role during capacitation, hyperactivation, acrosome reaction, and oocyte interaction (Tardif, Dube, Chevalier, & Bailey, 2001; Urner, Leppens-Luisier, & Sakkas, 2001; Sakkas et al., 2003; De Jonge, 2017).

Otherwise, post-translational modifications are also involved in the stability of microtubules and in regulating microtubules interactions with proteins (Kierszenbaum, 2002). Thus, a proper microtubules organization during spermatogenesis (Tachibana et al., 2005; O'Donnell & O'Bryan, 2014) and subsequent post-translational changes will influence on spermatozoa motility and hyperactivation during capacitation (Gagnon et al., 1996). The axoneme is composed of two central microtubules surrounded by nine microtubule doublets (9+2) which, in turn, are formed by heterodimers of α- and β-tubulins (Eddy, 2006). Tubulin is a polymorphic protein and results from the expression of various isogenes. Particularly, α-tubulin isoforms are TUBA1A, TUBA1B, TUBA3C, TUBA4A, TUBA4B, and TUBA8 (Khodiyar et al., 2007).

It is known that in human spermatozoa tubulin is one of the proteins that serve as substrate for post-transcriptional during spermatozoa epididymal maturation and capacitation, including tyrosine phosphorylation, mainly in the C-terminal structural domains of tubulin subunits (Ludueña, 1997; Westermann & Weber, 2003; Arcelay, Salicioni, Wertheimer, & Visconti, 2008). Specifically, tyrosine phosphorylation play roles in microtubule functions, such as microtubule stability, the interaction with associated proteins and the participation in axonemal motility (Gagnon et al., 1996; Garnham & Roll-Mecak, 2012; O'Donnell & O'Bryan, 2014). However, there is no data regarding the simultaneous study of both molecular events in the flagellum of the human spermatozoa. Here, we have addressed, for the first time, the relationship of flagellar tyrosine phosphorylation and α-tubulin (TUBA4A) distribution patterns in different spermatozoa physiological conditions.

Specially, we analysed the colocalization of these two biomarkers before capacitation, during one and four hours of capacitation, and after the induction of acrosome reaction in human spermatozoa.

2. RESULTS AND DISCUSSION

2.1 Spermatozoa parameters

All samples included in this study were normozoospermic according with WHO standards (Organization, 2010). Results of basic spermatozoa parameters from all physiological conditions (NC, C1, C4, AR1, and AR4) are summarized in the Table 1. We detected after both capacitation times and acrosome reaction induction (C1, C4, AR1, and AR4) a significant decrease in spermatozoa concentration (p <0.001) and an increase in motility and vitality (p<0.001) compared to NC cells (Table 1).

2.2 Assessment of acrosomal status

Acrosome reaction is an essential physiological event for the interaction and fusion of the spermatozoa with the oocyte (Mahi & Yanagimachi, 1978; Yanagimachi, 1994). In this study, the spermatozoa that fluoresced in the acrosomal region were regarded as not reacted and those with a label in the equatorial segment were considered reacted (see Figure 1). Results showed that in AR1 subpopulation the percentage of reacted cells was 67.6%, while only 12.1% of spontaneous reacted spermatozoa were observed in control (p<0.001; Table 1). Similarly, in AR4, 68.7% of cells exhibited positive acrosome reaction, compared to 15.7% from spontaneous acrosome reaction (p <0.001). No differences were found in the fractions of spontaneous and inducted acrosome-reacted

cells between both capacitation times (see Table 1). These data complement previous studies showing that the percentage of acrosome-reacted spermatozoa depends on the induction time (Sosa et al., 2014), and the percentage of cells with spontaneous acrosome reaction is around 20% (Cardona Maya, Olivera Angel, & Cadavid, 2006).

2.3 Tyrosine phosphorylation immunofluorescence

The molecular event of tyrosine phosphorylation is used as a spermatozoa capacitation indicator, since its presence has been associated with hyperactivation, cumulus oophorous penetration, and zona pellucida binding (Sakkas et al., 2003). We distinguished the phosphorylated state based on the positive label in the flagellum or the absence of it (see Figure 2a). Our immunofluorescence results showed that the percentage of spermatozoa with tyrosine phosphorylation at the flagellum increased from 8.4% to 18.3% ($P>0.05$) and 28.3% ($P<0.05$) after one- and four-hours capacitation, respectively. After the induction of acrosomal reaction, the number of phosphorylated spermatozoa rose up to 35.2% in AR1 and 49.2% in AR4. These percentages were significant different compared to noncapacitated and one-hour capacitated conditions (see Table 1).

Overall, our data indicate that longer capacitation times positively favoured the presence of tyrosine phosphorylation, with a higher percentage of phosphorylated cells after four-hours capacitation. These results are in accordance with previous studies performed in human (Barbonetti et al., 2008; Battistone et al., 2014) and in other mammalian species (Si & Okuno, 1999; Urner, Leppens-Luisier, & Sakkas, 2001) in which tyrosine phosphorylation increased in a time-related manner (Hereng et al., 2011; Liu, Clarke, & Baker, 2006; Martinez-Leon et al., 2015; Nassar et al., 1999).

2.4 α-tubulin immunofluorescence

Another essential requirement for proper spermatozoa motility is the adequate disposition of the

microtubules, which are composed mainly of tubulin (O'Donnell & O'Bryan, 2014). Moreover, it should be noted that the presence of structural defects in the axonema is one of the causes of male infertility in humans (Baccetti, Bruni, Gambera, Moretti, & Piomboni, 2004; Baccetti, Burrini, & Pallini, 1980; Gómez-Torres, Medrano, Romero, Fernandez-Colom, & Aizpurua, 2017; Peknicova et al., 2007).

We characterized four α-tubulin fluorescent patterns (see Figure 2b). Pattern 1 (P1) consisted of continuous label throughout the flagellum. Pattern 2 (P2) had discontinuous fluorescence along the whole flagellum. Pattern 3 (P3) was characterized by positive signal in terminal piece of the flagellum. Finally, Pattern 4 (P4) was classified as absence of labelling. Some of these patterns coinciding with patterns observed in previous studies (Draber, Draberova, & Viklicky, 1991; Francou, Ten, Bernabeu, & De Juan, 2014). This data highlights the existence of spermatozoa subpopulations with different α-tubulin distribution patterns.

We theorise that the post-translational modifications (Garnham & Roll-Mecak, 2012) could be hiding the α-tubulin epitopes, leading to the different fluorescent patterns observed. In addition, our data highlighted that spermatozoa capacitation increased the percentage of cells with α-tubulin distribution homogeneously throughout the flagellum (P1). This pattern also increased in cells after acrosomal reaction induction. Therefore, we propose that these physiological events could be helping to unmask the α-tubulin epitopes. Similarly, previous reports have also detected rearrangements of tubulin epitopes after acrosomal reaction in spermatozoa head and flagellum of several mammals (Dvorakova, Moore, Sebkova, & Palecek, 2005; Dvorakova, Palecek, & Peknicova, 2001; Peknicova et al., 2001). These observations support the image of axonema proteins as highly dynamic structure that participates actively in fertilization process (Wloga, Joachimiak, & Fabczak, 2017).

Specifically, low immunofluorescence scores of tubulin in spermatozoa has been related to low motility and low fertilizing potential, suggesting a possible structural or functional disorder in

the main axonema proteins (Hoshi, Sugano, Yoshimatsu, & Yanagida, 1995; Senn, Germond, & De Grandi, 1992). Other previous reports have found that the immunostaining of β-tubulin was less intense in pathological spermatozoa samples compared with normozoospermic ones (Baccetti et al., 2004; Salvolini et al., 2013). Additionally, in the complete form of fibrous sheath dysplasia the majority of spermatozoa (~50%) showed the tubulin label only over the final portion of the flagellum (P3), the second distribution (20–30%) consisted of a discontinuous signal (P2) and a continuous staining (P1), reminiscent of the normal pattern was detected in 15–30% of sperm tails (Rawe, Galaverna, Acosta, Olmedo, & Chemes, 2001). These studies reveal the importance of bright tubulin immunofluorescence throughout the flagellum (P1) for proper sperm functionality.

2.5 Simultaneous assessment of tyrosine phosphorylation and α-tubulin

The present study was aimed at establishing the Pearson correlation coefficient (PCC) between tyrosine phosphorylation and α-tubulin patterns by indirect simultaneous immunofluorescence in different spermatozoa physiological conditions (see Figure 2 and Figure 3). The PCC results showed that the distribution patterns of α-tubulin were dependent on the state of spermatozoa phosphorylation (see Figure 3 and Table 2). In particular, it is important to highlight that the presence of continuous α-tubulin pattern (P1) was significantly positively correlated (PCC; $p<0.01$) with tyrosine phosphorylation subpopulation and significantly negatively correlated (PCC; $p<0.01$) with unphosphorylated spermatozoa of all physiological conditions (NC, C1, C4, AR1, and AR4) (see Table 2). Therefore, P1 was the majoritarian pattern in all phosphorylated spermatozoa conditions (Figure 2d and Figure 3). In this line, a previous study claimed that α-tubulin acetylation is reduced in individuals with low spermatozoa motility (Bhagwat et al., 2014). In addition, a previous report observed that the absence of tubulin labeling in the flagellum could be associated with aberrant protein post-modification in different regions of the axoneme, affecting microtubules structure (Chan et al., 2009). Therefore, spermatozoa physiological events during fertilization such

as capacitation and acrosomal reaction are intimately linked with post- translational modifications and with the α-tubulin epitopes unmasking (Wloga et al., 2017).

Otherwise, we registered that spermatozoa with discontinuous α-tubulin pattern (P2) showed a positive and significant correlation (PCC; $p<0.05$) in NC regardless of phosphorylation status (Table 2). However, after both capacitation times and acrosomal reaction, phosphorylated spermatozoa presented a negative correlation with P2. Regarding terminal piece pattern (P3) and absence of labelling (P4), both patterns were negative correlated with phosphorylated spermatozoa subpopulation and positive correlated with nonphosphorylated cells of all physiological conditions (see Table 2). It should be noted that in the presence of tyrosine phosphorylation, the results did not record any spermatozoon without tubulin labeling (P4), due to this there is no representative image in Figure 2c. In nonphosphorylated cells, the most abundant distribution pattern of the α-tubulin varied according to the physiological state of the cells. In detail, spermatozoa from NC, C1, and C4 unphosphorylated conditions showed a higher percentage of P2, whereas, after the acrosome reaction induction (AR1 and AR4) presented mainly P3 (Figure 2d), which could be associated with alterations in flagellar motility. In this context, a previous report observed that after spermatozoa thawing the progressive motility was decreased as P3 α-tubulin pattern increased, indicating a tubulin disorganization (Gómez-Torres, Medrano, Romero, Fernandez-Colom, & Aizpurua, 2017).

In conclusion, this study reports for the first time a differential distribution of α-tubulin epitopes along the flagellum conditioned by the tyrosine phosphorylation state in human spermatozoa. Furthermore, the presented data demonstrate that longer capacitation times (four hours) and acrosome reaction allow selecting a subpopulation with greater percentage of phosphorylated spermatozoa linked to α-tubulin continuous distribution along the flagellum. Hence, these biomarkers could provide a new research tool for study the biological basis of infertility and the improvement of human spermatozoa selection methods in assisted reproduction.

3. MATERIALS AND METHODS

3.1 Experimental design

This research was approved by the ethical committee of the University of Alicante in accordance with the Declaration of Helsinki principles. Semen samples were processed following the experimental design (see Figure 4) to obtain the five selected spermatozoa physiological conditions: noncapacitated (NC), one hour capacitated (C1), four hours capacitated (C4), induced acrosome reaction from one hour capacitated (AR1), and induced acrosome reaction from four hours capacitated (AR4). C1 condition was chosen in concordance with the World Health Organization (WHO) swim-up protocol (Organization, 2010) and C4 based on a previous study (Baibakov et al., 2012). Cells from all conditions were fixed in 2% (*w/v*) paraformaldehyde (TAAB Essentials for Microscopy, UK) for 45 minutes at 4°C and then the simultaneous study of α-tubulin and tyrosine phosphorylation was performed.

3.2 Analysis of seminal parameters

Semen samples were obtained from five healthy normozoospermic donors by masturbation after three-to-four days of sexual abstinence under written informed consent. The samples were allowed to liquefy for 15 minutes at room temperature and basic seminogram was performed in the laboratory of the Department of Biotechnology at University of Alicante. Basic seminogram was performed mostly by following the WHO guidelines (Organization, 2010). Spermatozoa concentration and motility were assessed using Makler® (BioCare Europe, Rome, Italy) counting chamber, morphology by Papanicolaou staining (Panreac Química S.L.U., Barcelona, Spain), and viability was studied using eosin-nigrosine assay (Projectes i Serveis R+D S.L., Paterna, Spain). Only normozoospermic samples were included based on the criteria established by the WHO

(Organization, 2010).

3.3 In vitro capacitation by swim-up

The seminal plasma was removed by centrifugation for 10 minutes at 250g, the pellet was washed with human tubal fluid medium (HTF, Origio®, Måløv, Denmark) and divided into three aliquots, one to fix the noncapacitated spermatozoa and the others were destined for one and four hours capacitation. The capacitation was performed by swim-up using HTF medium supplemented with 5mg/mL of bovine serum albumin (BSA, Sigma-Aldrich®, Saint Louis, Missouri, USA) at 37ºC and 5.5% (*v*/v) of CO_2 for one and four hours. Next, supernatant fraction was collected and washed three times in phosphate buffered saline without calcium and magnesium (PBS, Biowest, Nuaillé, France) by centrifugation (250g, 10 minutes). All *in vitro* capacitation conditions were performed according to WHO (Organization, 2010). Following the capacitation, the concentration, motility, and viability of each motile spermatozoa recovery was analysed.

3.4 Induction and evaluation of acrosomal reaction

After the respective capacitation times, the supernatant of the tubes was collected and divided into three aliquots: one for the fixation of the capacitated spermatozoa, another for the induction of the acrosome reaction, and the last one as a control of the reaction. The induction of the acrosome reaction was performed by 10µM of calcium ionophore A23187 (Sigma-Aldrich) and 2mM of calcium chloride (Panreac Química S.L.U, Barcelona, Spain) for one hour at 37ºC and 5.5% (*v*/v) CO_2, following previous protocols (Cross, Morales, Overstreet, & Hanson, 1986). Only calcium chloride was added to the controls.

To assess the acrosomal status, 5µL of each physiological condition were placed on coverslips and fixed in methanol for 30 minutes. After the smear was dry, cells were washed three times in PBS and unspecific bindings were blocked using 2% (*w*/v) BSA-PBS for 30 minutes. The

smears were then incubated in the dark with *Pisum sativum agglutinin* lectin conjugated with fluorescein-5-isothiocyanate (PSA-FITC, Sigma-Aldrich) at a concentration of 50µg/mL for 30 minutes. After three washes in PBS, samples were mounted using Vectashield® and 4′,6-diamidine-2′-phenylindole dihydrochloride (DAPI, Vector Laboratories, Burlingame, California, USA). DAPI was used to detect the nucleus of the cells and the whole process was conducted at room temperature. A minimum of 200 spermatozoa of each experimental condition were evaluated using a confocal microscope (Zeiss LSM 800, Oberkochen, Germany).

3.5 Simultaneous immunolocation of tyrosine phosphorylation and α-tubulin

A total of 5µL of each paraformaldehyde-fixed condition were placed on a coverslip. When smear was dry, cells were washed three times for 5 minutes with PBS. Smears were then incubated with the primary PY20 anti-phosphotyrosine antibody (1:500) produced in rabbit (Sigma-Aldrich) in blocking solution of 2% PBS-BSA for one hour at room temperature (Barbonetti et al., 2008). Subsequently, three washes were made with PBS and the secondary anti-rabbit antibody conjugated with Alexa Fluor 488 (1:100) (Jackson ImmunoResearch, Ely, UK) was added in blocking solution of 2% (*w*/v) PBS-BSA for one hour at room temperature. Three washes were performed again and the primary anti-α-tubulin antibody (1:600) produced in mice (TUBA4A, Sigma-Aldrich) in blocking solution of 2% (*w*/v) PBS-BSA was added under the same conditions as previously. After washing, they were incubated with the secondary anti-mouse IgG (H+L) antibody conjugated to Cyanine ™3 (1:400) (Jackson ImmunoResearch) in blocking solution of 2% (*w*/v) PBS-BSA, under the same conditions. Finally, three washes were made with PBS and the assembly was carried out with Vectashield with DAPI.

Samples were visualized using a ZEISS LSM 800 confocal microscope, immunofluorescence is an alternative method to describe spermatozoa biomarkers, since it allows visualizing the relocation of molecules involved in the fertilization process (Sáez-Espinosa et al.,

2019). In each sample and in all the physiological conditions, a minimum of 100 cells were evaluated, therefore a total of 2,500 cells have been studied in this work. First, the presence or absence of phosphorylation was determined from each cell and afterwards, its distribution pattern of α-tubulin was identified.

3.6 Data collection and statistical analysis

Shapiro-Wilk (W) test was performed in order to test the distribution and equal variance in the biomarkers analysed, showing that all the biomarkers studied were normally distributed (W=0.806 to 0.956; $P>0.05$). Statistical tests were performed using the independent-samples t-test to assess differences in the biomarker's percentages between the different physiological conditions. The bivariate correlation between tyrosine phosphorylation and tubulin patterns in all groups was conducted using the Pearson correlation coefficient (PCC). Two-sided P -values<0.05 were deemed statistically significant and statistical analyses were performed using IBM SPSS Statistics 22.0 (IBM, Armonk, NY, USA).

AUTHORS' CONTRIBUTION

PSE, MFR, NHR, and LRG performed the experiments and collected the data. PSE, MFR, NHR, AR, and MJGT performed data analyses. JA, AR, and MJGT conceived the experimental design. All authors contributed to the drafting and approved the manuscript.

CONFLICTS OF INTEREST

The authors declare no conflicts of interest.

DATA AVAILABILITY STATEMENT

The authors confirm that the data supporting the findings of this study are available within the article. If you need further information, please contact the author correspondence, MJGT.

REFERENCES

Arcelay, E., Salicioni, A. M., Wertheimer, E., & Visconti, P. E. (2008). Identification of proteins undergoing tyrosine phosphorylation during mouse sperm capacitation. *The International Journal of Developmental Biology*, *52*(5–6), 463–472. https://doi.org/10.1387/ijdb.072555ea [doi]

AUSTIN, C. R. (1951). Observations on the penetration of the sperm in the mammalian egg. *Australian Journal of Scientific Research.Ser.B: Biological Sciences*, *4*(4), 581–596.

AUSTIN, C. R. (1952). The capacitation of the mammalian sperm. *Nature*, *170*(4321), 326.

Baccetti, B., Bruni, E., Gambera, L., Moretti, E., & Piomboni, P. (2004). An ultrastructural and immunocytochemical study of a rare genetic sperm tail defect that causes infertility in humans. *Fertility and Sterility*, *82*(2), 463–468. https://doi.org/10.1016/j.fertnstert.2003.12.049 [doi]

Baccetti, B., Burrini, A. G., & Pallini, V. (1980). Spermatozoa and cilia lacking axoneme in an infertile man. *Andrologia*, *12*(6), 525–532.

Baibakov, B., Boggs, N. A., Yauger, B., Baibakov, G., & Dean, J. (2012). Human sperm bind to the N-terminal domain of ZP2 in humanized zonae pellucidae in transgenic mice. *The Journal of Cell Biology*, *197*(7), 897–905. https://doi.org/10.1083/jcb.201203062 [doi]

Barbonetti, A., Vassallo, M. R., Cinque, B., Antonangelo, C., Sciarretta, F., Santucci, R., … Francavilla, F. (2008). Dynamics of the global tyrosine phosphorylation during capacitation and acquisition of the ability to fuse with oocytes in human spermatozoa. *Biology of Reproduction*, *79*(4), 649–656. https://doi.org/10.1095/biolreprod.108.068254 [doi]

Battistone, M. A., Alvau, A., Salicioni, A. M., Visconti, P. E., Da Ros, V. G., & Cuasnicu, P. S. (2014). Evidence for the involvement of proline-rich tyrosine kinase 2 in tyrosine phosphorylation downstream of protein kinase A activation during human sperm capacitation. *Molecular Human Reproduction*, *20*(11), 1054–1066. https://doi.org/10.1093/molehr/gau073 [doi]

Bhagwat, S., Dalvi, V., Chandrasekhar, D., Matthew, T., Acharya, K., Gajbhiye, R., … Parte, P. (2014). Acetylated alpha-tubulin is reduced in individuals with poor sperm motility. *Fertility and Sterility*, *101*(1), 95-104.e3. https://doi.org/10.1016/j.fertnstert.2013.09.016 [doi]

Brohi, R. D., & Huo, L.-J. (2017). Posttranslational Modifications in Spermatozoa and Effects on Male Fertility and Sperm Viability. *Omics : A Journal of Integrative Biology*, *21*(5), 245–256. https://doi.org/10.1089/omi.2016.0173

Buffone, M. G., Doncel, G. F., Marin Briggiler, C. I., Vazquez-Levin, M. H., & Calamera, J. C. (2004). Human sperm subpopulations: relationship between functional quality and protein tyrosine phosphorylation. *Human Reproduction (Oxford, England)*, *19*(1), 139–146.

Buffone, M. G., Verstraeten, S. V, Calamera, J. C., & Doncel, G. F. (2009). High cholesterol content and decreased membrane fluidity in human spermatozoa are associated with protein tyrosine phosphorylation and functional deficiencies. *Journal of Andrology*, *30*(5), 552–558. https://doi.org/10.2164/jandrol.108.006551 [doi]

Cardona Maya, W. D., Olivera Angel, M., & Cadavid, A. P. (2006). [Evaluation of the calcium ionophore induced acrosome reaction: a more realistic approach to the fecundant capacity of the spermatozoid]. *Archivos espanoles de urologia*, *59*(5), 501–510. https://doi.org/10.4321/s0004-06142006000500007

Chan, C. C., Shui, H. A., Wu, C. H., Wang, C. Y., Sun, G. H., Chen, H. M., & Wu, G. J. (2009). Motility and protein phosphorylation in healthy and asthenozoospermic sperm. *Journal of Proteome Research*, *8*(11), 5382–5386. https://doi.org/10.1021/pr9003932 [doi]

CHANG, M. C. (1951). Fertilizing capacity of spermatozoa deposited into the fallopian tubes. *Nature*, *168*(4277), 697–698.

Cross, N. L., Morales, P., Overstreet, J. W., & Hanson, F. W. (1986). Two simple methods for detecting acrosome-reacted human sperm. *Gamete Research*, *15*(3), 213–226. https://doi.org/10.1002/mrd.1120150303

De Jonge, C. (2017). Biological basis for human capacitation-revisited. *Human Reproduction Update*, *23*(3), 289–299. https://doi.org/10.1093/humupd/dmw048 [doi]

de Lamirande, E., Leclerc, P., & Gagnon, C. (1997). Capacitation as a regulatory event that primes spermatozoa for the acrosome reaction and fertilization. *Molecular Human Reproduction*, *3*(3), 175–194.

Draber, P., Draberova, E., & Viklicky, V. (1991). Immunostaining of human spermatozoa with tubulin domain-specific monoclonal antibodies. Recognition of a unique beta-tubulin epitope in the sperm head. *Histochemistry*, *95*(5), 519–524. https://doi.org/10.1007/bf00315749 [doi]

Dvorakova, K., Moore, H. D., Sebkova, N., & Palecek, J. (2005). Cytoskeleton localization in the sperm head prior to fertilization. *Reproduction (Cambridge, England)*, *130*(1), 61–69. https://doi.org/130/1/61 [pii]

Dvorakova, K., Palecek, J., & Peknicova, J. (2001). Changes in immunocytochemical localization of cytoskeletal proteins in boar spermatozoa after acrosome reaction induced by specific cytoskeletal inhibitors. *Folia Biologica*, *47*(1), 18–27.

Eddy, E. M. (2006). CHAPTER 1 - The Spermatozoon Gamete Biology Section, Laboratory of Reproductive and Developmental Toxicology, National Institute of Environmental Health Sciences, National Institutes of Health, Research Triangle Park, North Carolina. In J. D. B. T.-K. and N. P. of R. (Third E. Neill (Ed.) (pp. 3–54). St Louis: Academic Press. https://doi.org/https://doi.org/10.1016/B978-012515400-0/50006-3

Edwards, R. G., Bavister, B. D., & Steptoe, P. C. (1969). Early stages of fertilization in vitro of human oocytes matured in vitro. *Nature*, *221*(5181), 632–635.

Francou, M. M., Ten, J., Bernabeu, R., & De Juan, J. (2014). Capacitation and acrosome reaction changes α-tubulin immunodistribution in human spermatozoa. *Reproductive BioMedicine Online*. https://doi.org/https://doi.org/10.1016/j.rbmo.2013.10.001

Gagnon, C., White, D., Cosson, J., Huitorel, P., Edde, B., Desbruyeres, E., … Cibert, C. (1996). The polyglutamylated lateral chain of alpha-tubulin plays a key role in flagellar motility. *Journal of Cell Science*, *109 (Pt 6*(Pt 6), 1545–1553.

Garnham, C. P., & Roll-Mecak, A. (2012). The chemical complexity of cellular microtubules: tubulin post-translational modification enzymes and their roles in tuning microtubule functions. *Cytoskeleton (Hoboken, N.J.)*, *69*(7), 442–463. https://doi.org/10.1002/cm.21027 [doi]

Gomez-Torres, M. J., Medrano, L., Romero, A., Fernandez-Colom, P. J., & Aizpurua, J. (2017). Effectiveness of human spermatozoa biomarkers as indicators of structural damage during cryopreservation. *Cryobiology*, *78*, 90–94. https://doi.org/S0011-2240(17)30060-3 [pii]

Hereng, T. H., Elgstoen, K. B., Cederkvist, F. H., Eide, L., Jahnsen, T., Skalhegg, B. S., & Rosendal, K. R. (2011). Exogenous pyruvate accelerates glycolysis and promotes capacitation in human spermatozoa. *Human Reproduction (Oxford, England)*, *26*(12), 3249–3263. https://doi.org/10.1093/humrep/der317 [doi]

Hoshi, K., Sugano, T., Yoshimatsu, N., & Yanagida, K. (1995). Correlation of semen characteristics with acrosin, hyaluronidase, tubulin, dynein, and actin of spermatozoa. *Archives of Andrology*, *35*(3), 165–172. https://doi.org/10.3109/01485019508987869 [doi]

Khodiyar, V. K., Maltais, L. J., Ruef, B. J., Sneddon, K. M., Smith, J. R., Shimoyama, M., … Lovering, R. C. (2007). A revised nomenclature for the human and rodent alpha-tubulin gene family. *Genomics*, *90*(2), 285–289. https://doi.org/S0888-7543(07)00097-3 [pii]

Kierszenbaum, A. L. (2002). Sperm axoneme: a tale of tubulin posttranslation diversity. *Molecular Reproduction and Development*, *62*(1), 1–3. https://doi.org/10.1002/mrd.10139 [doi]

Liu, D. Y., Clarke, G. N., & Baker, H. W. (2006). Tyrosine phosphorylation on capacitated human sperm tail detected by immunofluorescence correlates strongly with sperm-zona pellucida (ZP) binding but not with the ZP-induced acrosome reaction. *Human Reproduction (Oxford, England)*, *21*(4), 1002–1008. https://doi.org/dei435 [pii]

Ludueña, R. F. (1997). Multiple Forms of Tubulin: Different Gene Products and Covalent Modifications. (K. W. Jeon, Ed.), *International Review of Cytology*. Academic Press. https://doi.org/https://doi.org/10.1016/S0074-7696(08)62138-5

Mahi, C. A., & Yanagimachi, R. (1978). Capacitation, acrosome reaction, and egg penetration by canine spermatozoa in a simple defined medium. *Gamete Research*, *1*(2), 101–109. https://doi.org/10.1002/mrd.1120010203

Martinez-Leon, E., Osycka-Salut, C., Signorelli, J., Pozo, P., Perez, B., Kong, M., … Diaz, E. S. (2015). Fibronectin stimulates human sperm capacitation through the cyclic AMP/protein kinase A pathway. *Human Reproduction (Oxford, England)*, *30*(9), 2138–2151. https://doi.org/10.1093/humrep/dev154 [doi]

Naresh, S., & Atreja, S. K. (2015). The protein tyrosine phosphorylation during in vitro capacitation and cryopreservation of mammalian spermatozoa. *Cryobiology*, *70*(3), 211–216. https://doi.org/10.1016/j.cryobiol.2015.03.008 [doi]

Nassar, A., Mahony, M., Morshedi, M., Lin, M. H., Srisombut, C., & Oehninger, S. (1999). Modulation of sperm tail protein tyrosine phosphorylation by pentoxifylline and its correlation with hyperactivated motility. *Fertility and Sterility*, *71*(5), 919–923. https://doi.org/S0015-0282(99)00013-8 [pii]

Naz, R. K., & Rajesh, P. B. (2004). Role of tyrosine phosphorylation in sperm capacitation / acrosome reaction. *Reproductive Biology and Endocrinology : RB&E*, *2*, 75. https://doi.org/1477-7827-2-75 [pii]

O'Donnell, L., & O'Bryan, M. K. (2014). Microtubules and spermatogenesis. *Seminars in Cell & Developmental Biology*, *30*, 45–54. https://doi.org/10.1016/j.semcdb.2014.01.003 [doi]

Organization, W. H. (2010). WHO laboratory manual for the examination and processing of human semen. World Health Organization.

Ostermeier, G. C., Cardona, C., Moody, M. A., Simpson, A. J., Mendoza, R., Seaman, E., & Travis, A. J. (2018). Timing of sperm capacitation varies reproducibly among men. *Molecular Reproduction and Development*, *85*(5), 387–396. https://doi.org/10.1002/mrd.22972 [doi]

Patel, A. S., Leong, J. Y., & Ramasamy, R. (2018). Prediction of male infertility by the World Health Organization laboratory manual for assessment of semen analysis: A systematic review. *Arab Journal of Urology*, *16*(1), 96–102. https://doi.org/10.1016/j.aju.2017.10.005

Peknicova, J., Kubatova, A., Sulimenko, V., Draberova, E., Viklicky, V., Hozak, P., & Draber, P. (2001). Differential subcellular distribution of tubulin epitopes in boar spermatozoa: recognition of class III beta-tubulin epitope in sperm tail. *Biology of Reproduction*, *65*(3), 672–679. https://doi.org/10.1095/biolreprod65.3.672 [doi]

Peknicova, J., Pexidrova, M., Kubatova, A., Koubek, P., Tepla, O., Sulimenko, T., & Draber, P. (2007). Expression of beta-tubulin epitope in human sperm with pathological spermiogram. *Fertility and Sterility*, *88*(4 Suppl), 1120–1128. https://doi.org/S0015-0282(07)00105-7 [pii]

Rawe, V. Y., Galaverna, G. D., Acosta, A. A., Olmedo, S. B., & Chemes, H. E. (2001). Incidence of tail structure distortions associated with dysplasia of the fibrous sheath in human spermatozoa. *Human Reproduction*, *16*(5), 879–886. https://doi.org/10.1093/humrep/16.5.879

Saez-Espinosa, P., Huerta-Retamal, N., Robles-Gomez, L., Aviles, M., Aizpurua, J., Velasco, I., … Gomez-Torres, M. J. (2019). Influence of in vitro capacitation time on structural and functional human sperm parameters. *Asian Journal of Andrology*. https://doi.org/10.4103/aja.aja_104_19 [doi]

Sakkas, D., Leppens-Luisier, G., Lucas, H., Chardonnens, D., Campana, A., Franken, D. R., & Urner, F. (2003). Localization of tyrosine phosphorylated proteins in human sperm and relation to capacitation and zona pellucida binding. *Biology of Reproduction*, *68*(4), 1463–1469. https://doi.org/10.1095/biolreprod.102.011023 [doi]

Salvolini, E., Buldreghini, E., Lucarini, G., Vignini, A., Lenzi, A., Di Primio, R., & Balercia, G. (2013). Involvement of sperm plasma membrane and cytoskeletal proteins in human male infertility. *Fertility and Sterility*, *99*(3), 697–704. https://doi.org/10.1016/j.fertnstert.2012.10.042 [doi]

Senn, A., Germond, M., & De Grandi, P. (1992). Immunofluorescence study of actin, acrosin, dynein, tubulin and hyaluronidase and their impact on in-vitro fertilization. *Human Reproduction (Oxford, England)*, *7*(6), 841–849. https://doi.org/10.1093/oxfordjournals.humrep.a137747 [doi]

Si, Y., & Okuno, M. (1999). Role of tyrosine phosphorylation of flagellar proteins in hamster sperm hyperactivation. *Biology of Reproduction*, *61*(1), 240–246.

Sosa, C. M., Pavarotti, M. A., Zanetti, M. N., Zoppino, F. C. M., De Blas, G. A., & Mayorga, L. S. (2014). Kinetics of human sperm acrosomal exocytosis. *Molecular Human Reproduction*, *21*(3), 244–254. https://doi.org/10.1093/molehr/gau110

Tachibana, M., Terada, Y., Murakawa, H., Murakami, T., Yaegashi, N., & Okamura, K. (2005). Dynamic changes in the cytoskeleton during human spermiogenesis. *Fertility and Sterility*, *84 Suppl 2*, 1241–1248. https://doi.org/S0015-0282(05)01442-1 [pii]

Tardif, S., Dube, C., Chevalier, S., & Bailey, J. L. (2001). Capacitation is associated with tyrosine phosphorylation and tyrosine kinase-like activity of pig sperm proteins. *Biology of Reproduction*, *65*(3), 784–792.

Urner, F., Leppens-Luisier, G., & Sakkas, D. (2001). Protein tyrosine phosphorylation in sperm during gamete interaction in the mouse: the influence of glucose. *Biology of Reproduction*, *64*(5), 1350–1357.

Visconti, P. E., Galantino-Homer, H., Moore, G. D., Bailey, J. L., Ning, X., Fornes, M., & Kopf, G. S. (1998). The molecular basis of sperm capacitation. *Journal of Andrology*, *19*(2), 242–248.

Westermann, S., & Weber, K. (2003). Post-translational modifications regulate microtubule function. *Nature Reviews.Molecular Cell Biology*, *4*(12), 938–947. https://doi.org/10.1038/nrm1260 [doi]

Wloga, D., Joachimiak, E., & Fabczak, H. (2017). Tubulin Post-Translational Modifications and Microtubule Dynamics. *International Journal of Molecular Sciences*, *18*(10). https://doi.org/10.3390/ijms18102207

Yanagimachi, R. (1994). Mammalian fertilization. In R. Press (Ed.), *The Physiologist of reproduction* (Vol. 1, pp. 189–317). Department of Anatomy and Reproductive Biology, University of Hawaii Medical School, Honolulu 96822, USA.: E. Knobil & J.D. Neill.

TABLES

TABLE 1 Semen sample parameters.

Parameter	NC Mean ± SD	C1 Mean ± SD	C4 Mean ± SD	AR1 Mean ± SD	AR4 Mean ± SD
Volume (mL)	4.4 ± 1.5	-	-	-	-
pH	7.6 ± 0.2	-	-	-	-
Normal morphology (%)	12.5 ± 5.4	-	-	-	-
Concentration (10^6/mL)	76.7 ± 32.8	15.4 ± 10.4[a]	19.0 ± 8.2[a]	15.4 ± 10.4[a]	19.0 ± 8.2[a]
Total motility (%)	65.2 ± 10.8	98.5 ± 1.9[a]	96.8 ± 2.7[a]	91.2 ± 3.6[a]	90.1 ± 5.4[a]
Viability (%)	84.2 ± 8.1	97.6 ± 2.1[a]	95.2 ± 2.1[a]	94.4 ± 4.5[a]	91.4 ± 3.2[a]
Acrosome reaction (%)	-	12.1 ± 8.8	15.7 ± 7.3	67.6 ± 13.7[b,c]	68.7 ± 14.7[b,c]
Tyrosine phosphorylation (%)	8.4 ± 3.8	18.3 ± 9.6	28.3 ± 13.9[a]	35.2 ± 8.5[a,b]	49.2 ± 18.0[a,b]

Noncapacitated (NC), one hour capacitated (C1), four hours capacitated (C4), acrosomal reaction inducted after one hour (AR1) and four hours of capacitation (AR4).
[a] t-test $p<0.001$to NC, [b] t-test $p<0.001$to C1, [c] t-test $p<0.001$to C4.

TABLE 2 Bivariate Pearson correlation between α-tubulin patterns (P1-P4) and tyrosine phosphorylated state (TP + or TP -) in each human spermatic physiological condition.

		PCC of α-Tubulin patterns			
	TP	**P1**	**P2**	**P3**	**P4**
NC	+	0.836**	0.745*	-0.583	-0.458
	-	-0.954**	0.822**	0.719*	0.570
C1	+	0.903**	-0.677*	-0.737*	-0.423
	-	-0.808**	0.417	0.869**	0.707*
C4	+	0.911**	-0.541	-0.831**	-0.593
	-	-0.943**	0.576	0.846**	0.623
AR1	+	0.852**	-0.633*	-0.691*	-0.398
	-	-0.784**	0.476	0.799**	0.526
AR4	+	0.793**	-0.523	-0.639*	-0.452
	-	-0.889**	0.643*	0.639*	0.700*

Pearson correlation coefficient (PCC), Noncapacitated (NC), one hour capacitated (C1), four hours capacitated (C4), acrosomal reaction inducted after one hour (AR1), four hours of capacitation (AR4), phosphorylated (TP+), and unphosphorylated (TP -). Note that the continuous α-tubulin pattern (P1) was significantly positively correlated with tyrosine phosphorylation subpopulation and

significantly negatively correlated with unphosphorylated spermatozoa of all physiological conditions.

* Significative correlation ($p<0.05$); ** Significative correlation ($p<0.01$).

FIGURE LEGENDS

FIGURE 1 Fluorescent PSA-FITC binding label. Acrosomal region label indicates absence of acrosome reaction and the labelling in the equatorial band that the acrosome reaction has been performed. (a) Spermatozoa before acrosome reaction induction. (b) Spermatozoa after acrosome reaction induction. Scale bar 10μm.

FIGURE 2 Immunocolocalization of α-tubulin and tyrosine phosphorylation in human spermatozoa flagellum. (A) Tyrosine phosphorylation, phosphorylated (+) and unphosphorylated spermatozoa (-). (B) Patterns of α-tubulin distribution, Homogeneous and continuous (P1), discontinuous (P2), terminal piece (P3), and no labelling (P4). (C) Patterns of colocalization biomarkers, phosphorylated cell with continuous α-tubulin labelling (P1+), phosphorylated cell with discontinuous α-tubulin labelling (P2+), and phosphorylated cell with α-tubulin labelling in the terminal piece (P3+). The DNA of the spermatozoa was stained with DAPI. Scale bar 10μm. (D) Spermatozoa percentages of simultaneous study of tyrosine phosphorylation (TP+, phosphorylated; TP -, unphosphorylated) and α-tubulin flagellar distribution (P1-P4) in each physiological condition (NC, C1, C4, AR1, and AR4).

FIGURE 3 Fluorescent immunocolocalization of α-tubulin and tyrosine phosphorylation in human spermatozoa flagellum in different experimental conditions. The DNA of the spermatozoa was stained with DAPI (magnitude 400x). Note that regardless of the experimental condition the spermatozoa with tyrosine phosphorylation localize tubulin homogeneously throughout the flagellum (P1).

FIGURE 4 Experimental design. Spermatozoa physiological conditions: Noncapacitated (NC), one-hour capacitated (C1), four-hour capacitated (C4), acrosomal reacted cells after one hour (AR1), and four hours of capacitation (AR4).

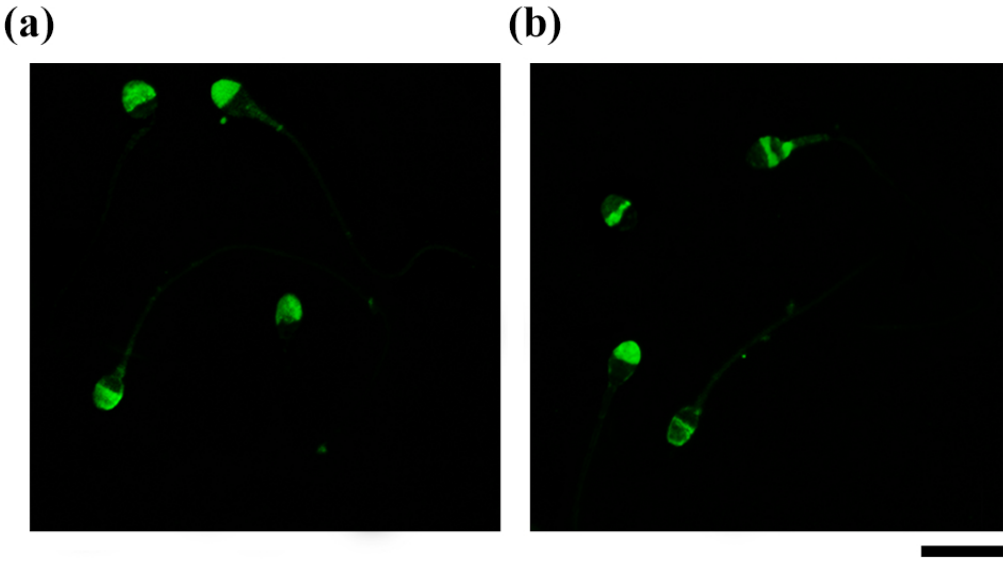

Fluorescent PSA-FITC binding label. Acrosomal region label indicates absence of acrosome reaction and the labelling in the equatorial band that the acrosome reaction has been performed. (a) Spermatozoa before acrosome reaction induction. (b) Spermatozoa after acrosome reaction induction. Scale bar 10μm.

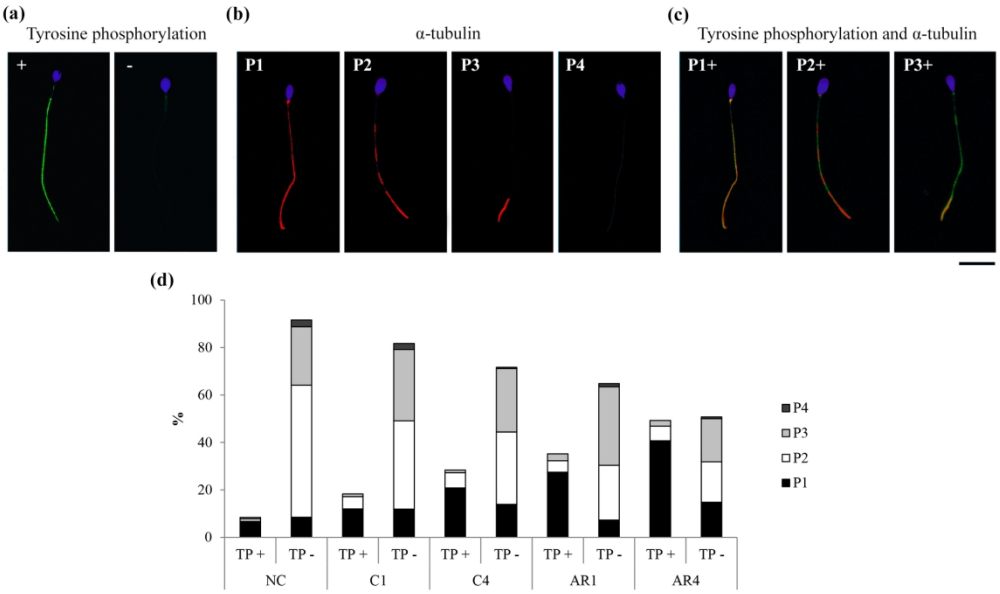

Immunocolocalization of α-tubulin and tyrosine phosphorylation in human spermatozoa flagellum. (A) Tyrosine phosphorylation, phosphorylated (+) and unphosphorylated spermatozoa (-). (B) Patterns of α-tubulin distribution, Homogeneous and continuous (P1), discontinuous (P2), terminal piece (P3), and no labelling (P4). (C) Patterns of colocalization biomarkers, phosphorylated cell with continuous α-tubulin labelling (P1+), phosphorylated cell with discontinuous α-tubulin labelling (P2+), and phosphorylated cell with α-tubulin labelling in the terminal piece (P3+). The DNA of the spermatozoa was stained with DAPI. Scale bar 10μm. (D) Spermatozoa percentages of simultaneous study of tyrosine phosphorylation (TP+, phosphorylated; TP -, unphosphorylated) and α-tubulin flagellar distribution (P1-P4) in each physiological condition (NC, C1, C4, AR1, and AR4).

180x107mm (300 x 300 DPI)

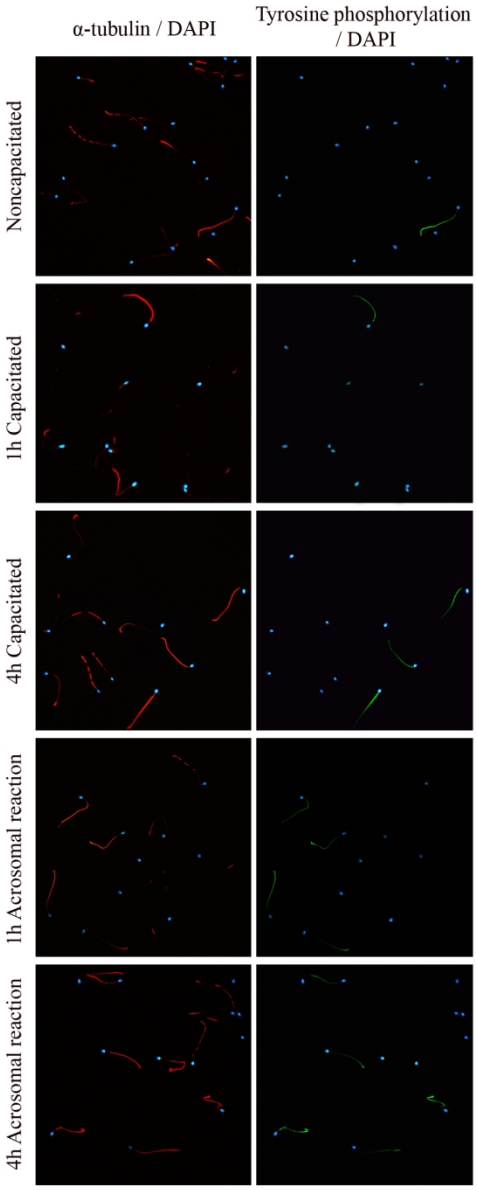

Fluorescent immunocolocalization of α-tubulin and tyrosine phosphorylation in human spermatozoa flagellum in different experimental conditions. The DNA of the spermatozoa was stained with DAPI (magnitude 400x). Note that regardless of the experimental condition the spermatozoa with tyrosine phosphorylation localize tubulin homogeneously throughout the flagellum (P1).

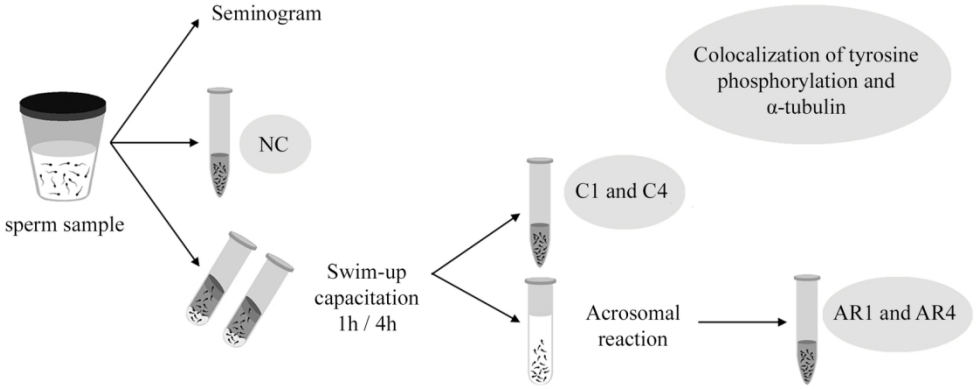

Experimental design. Spermatozoa physiological conditions: Noncapacitated (NC), one-hour capacitated (C1), four-hour capacitated (C4), acrosomal reacted cells after one hour (AR1), and four hours of capacitation (AR4).

146x59mm (300 x 300 DPI)